International Journal of Scientific Research in Engineering and Management (IJSREM)
Volume: 10 Issue: 04 | April - 2026 SJIF Rating: 8.659 ISSN: 2582-3930

Prediction of Mechanical Properties of 3D Printed Parts Using Machine Learning Techniques

SM. Sanaullah[1], V.V. Siva Satya Narayana[1], P. Satya Vardhan[1], Dr. V. Ramakoteswara Rao[2]

1 Department of Mechanical Engineering, RVR & JC College of Engineering, Guntur, Andhra Pradesh, India

2 Associate Professor, Department of Mechanical Engineering, RVR & JC College of Engineering, Guntur, Andhra Pradesh, India

Abstract

Additive manufacturing (AM), specifically Fused Deposition Modelling (FDM), is one of the most widely adopted fabrication technologies, enabling layer-by-layer construction of complex geometries with minimal material waste. The mechanical performance of FDM-fabricated components -- including tensile strength, hardness, surface roughness, and impact strength -- is critically dependent on process parameters such as layer thickness, printing speed, and infill density. This study presents a comprehensive machine learning (ML) based comparative framework for predicting four mechanical properties across three thermoplastic materials: ABS, PLA, and PETG. A full factorial design (27 runs per material) was employed. Eight ML algorithms -- ANN, KNN, LR, SVR, XG Boost, Bayesian Ridge, BPNN, and Random Forest -- were implemented in Python using Google Colab and evaluated using R2, MAE, MSE, and RMSE. Results show ANN achieved peak R2=0.9894 for PETG tensile strength and R2=0.9822 for ABS hardness. SVR was best for ABS impact test (R2=0.8928). These findings provide a validated ML-based optimization framework for FDM process parameter selection.

Keywords *— FDM; Machine Learning; ABS; PLA; PETG; ANN; SVR; XG Boost; Random Forest; Mechanical Properties.*

I. INTRODUCTION

Additive manufacturing (AM) has undergone a remarkable transformation from a rapid prototyping tool into a full-scale production technology over the past two decades [1]. Among AM techniques, Fused Deposition Modeling (FDM) is the most widely deployed method, owing to its low operational cost, broad material compatibility, and ease of use [2]. FDM operates by extruding a thermoplastic filament through a heated nozzle, depositing molten material layer by layer along toolpaths generated from a sliced digital model until the full geometry is formed.

The mechanical performance of FDM-fabricated parts remains highly sensitive to process parameter selection. Parameters including layer thickness, infill density, printing speed, nozzle temperature, raster angle, and bed temperature directly govern interlayer bonding quality, porosity, surface finish, and overall structural integrity [3]. Incorrect parameter selection can result in delamination, warping, poor dimensional accuracy, reduced tensile strength, and increased surface roughness -- all of which lead to part failure in functional applications.

Three thermoplastic materials dominate the FDM landscape: Acrylonitrile Butadiene Styrene (ABS), Polylactic Acid (PLA), and Polyethylene Terephthalate Glycol (PETG). ABS is widely used in engineering applications demanding high impact resistance, thermal stability, and dimensional accuracy. PLA is preferred for biodegradability, low printing temperature, and ease of use in prototyping settings. PETG combines chemical resistance and toughness with superior interlayer adhesion compared to PLA [4].

Machine learning (ML) has emerged as a powerful paradigm for data-driven modeling of complex manufacturing processes [5]. Previous studies [6-9] have demonstrated that ML algorithms such as neural networks, support vector machines, and ensemble methods can accurately predict mechanical properties of FDM parts from process parameters. However, a comprehensive multi-material, multi-algorithm comparative study predicting four mechanical properties simultaneously across ABS, PLA, and PETG remains a significant gap. This study addresses that gap.

II. LITERATURE REVIEW

The intersection of machine learning and additive manufacturing has attracted growing research interest, as reviewed by Wang et al. [5] and Kumar et al. [12]. These reviews confirm that neural networks, ensemble methods, and support vector machines consistently outperform traditional statistical models for mechanical property prediction in FDM processes.

Özkül et al. [6] applied 25 ML algorithms using the WEKA platform to predict hardness, tensile strength, flexural strength, and surface roughness of ABS FDM parts from 27 experimental samples. KSTAR achieved R2=0.9997 for hardness and MLP achieved R2=0.9999 for flexural strength. ANOVA analysis confirmed that infill density was the most dominant parameter for strength properties (55.56-80.02%), while layer thickness was most influential for surface roughness (70.89%).

Cerro et al. [7] predicted surface roughness of FDM parts using 40 trained models, identifying raster angle and layer height as most influential. Hooda et al. [8] used Random Forest with K-fold cross-validation to predict deposition angle, achieving 94.57% accuracy. Charalampous et al. [9] developed ML regression models predicting dimensional deviations between CAD models and fabricated FDM parts. Ulkir [10] applied SVR to model mechanical and electrical behavior of carbon black-filled ABS FDM parts.

Algarni and Ghazali [4] confirmed that each of ABS, PLA, PEEK, and PETG exhibits distinct parameter-property relationships requiring material-specific ML models. Despite these advances, a comprehensive comparison of eight ML algorithms across three different FDM materials simultaneously predicting four

mechanical properties remains a critical gap that the present study fills.

III. MATERIALS AND METHODS

A. Materials

Three thermoplastic filament materials were selected based on their commercial prevalence. ABS was selected for its high strength, impact resistance, and thermal resistance [4]. PLA was chosen for its biodegradability, ease of printing, and predictable mechanical behavior [37]. PETG was included for its superior chemical resistance, excellent layer adhesion, and intermediate mechanical properties between ABS and PLA [4]. All filaments were 1.75 mm diameter, sourced from the same commercial supplier batch.

B. Experimental Design

A full factorial experimental design (L27) was employed with three input parameters, each at three levels, resulting in 27 experimental combinations per material (3^3 = 27). The input parameters and their levels are summarized in TABLE I. All specimens were fabricated on a standard FDM printer with a 0.4 mm brass nozzle. Nozzle and bed temperatures: ABS (230 deg C / 100 deg C), PLA (210 deg C / 60 deg C), PETG (240 deg C / 80 deg C). Wall thickness (1.2 mm) and infill pattern (grid) were held constant. All measurements were averaged over five repetitions.

TABLE I.. Input Parameters and Level Values.

Parameter	Symbol	Units	Level 1	Level 2	Level 3
Layer Thickness	LT	mm	0.15	0.25	0.35
Printing Speed	PS	mm/s	40	60	80
Infill Density	ID	%	20	60	100

C. Measurement of Mechanical Properties

Four mechanical properties were measured with five repetitions averaged per specimen: (1) Tensile Strength (MPa) -- ASTM D638, universal testing machine, 1 mm/s crosshead speed; (2) Hardness (Shore D) -- ASTM D2240, five-point average, 1 kg/cm2 applied pressure; (3) Surface Roughness (Ra, um) -- contact profilometer, 2.5 mm sampling length, 0.75 mm/s traverse speed; (4) Impact Strength (J/m) -- Izod notched impact tester, ASTM D256. All tests at 23 deg C +/- 2 deg C, 50% +/- 5% RH.

D. Machine Learning Implementation

All models were implemented in Python 3.9 (Google Colab) using scikit-learn v1.2 and XGBoost v1.7. Inputs were normalized via StandardScaler. Ten-fold cross-validation with 75%/25% split was applied. The eight algorithms: (1) ANN -- hidden layers (100, 50), ReLU, Adam; (2) KNN -- K=5, Euclidean; (3) LR -- OLS baseline; (4) SVR -- RBF kernel, C=100, eps=0.1; (5) XG Boost -- 100 estimators, depth=6; (6) Bayesian Ridge -- auto regularization; (7) BPNN -- hidden layers (128, 64, 32), sigmoid, SGD; (8) RF -- 100 trees, max_features=sqrt.

E. Performance Evaluation Metrics

Model performance was assessed using R2 (coefficient of determination), MAE, MSE, and RMSE. R2 closer to 1.0 indicates superior predictive accuracy; negative R2 values indicate the model performs worse than a simple mean predictor -- a clear sign of overfitting on small datasets.

VI. EXPERIMENTAL DATASET

This section presents the complete experimental datasets for all three thermoplastic materials — ABS, PLA, and PETG — used in this study. Each dataset comprises 27 runs corresponding to a full factorial (L27) design with three input parameters (Layer Thickness, Printing Speed, Infill Density) and four measured output properties (Surface Roughness, Impact Strength, Tensile Strength, and Hardness). These datasets formed the basis for training and evaluating all eight machine learning models described in Section III. Descriptive statistics for each material are also provided to facilitate inter-material comparison.

A. ABS Dataset

TABLE VI presents the complete experimental data for ABS (Acrylonitrile Butadiene Styrene). ABS specimens were printed at a nozzle temperature of 230°C and bed temperature of 100°C. Surface roughness values ranged widely (299.48–673.70 Ra µm), reflecting strong sensitivity to layer thickness and printing speed. Impact strength showed moderate variation (104.74–141.43 J/m), while hardness remained relatively stable (61.06–72.02 Shore D), consistent with ABS's rigid polymer matrix. Tensile strength ranged from 18.97 to 26.65 MPa.

TABLE VI. Full Experimental Dataset — ABS Material (27 Runs, L27 Full Factorial).

Layer Thickness (mm)	Printing Speed (mm/s)	Infill Density (%)	Surface Roughness (Ra, µm)	Impact Strength (J/m)	Tensile Strength (MPa)	Hardness (Shore D)
0.15	60	30	455.29	104.74	22.47	68.52
0.15	40	45	624.5	120.82	20.42	67.92
0.15	40	30	550.69	112.65	21.37	69.65
0.35	40	15	308.94	121.75	21.28	68.12
0.15	40	15	402.67	116.36	22.04	72.02
0.35	40	45	590.4	141.43	19.03	62.75
0.25	80	30	500.89	116.12	21.19	63.81
0.35	60	15	328.66	119.1	20.64	67.42
0.15	80	30	420.22	112.96	23.87	64.16
0.25	60	30	521.6	108.65	20.56	68.09
0.15	60	15	359.36	111.29	21.98	70.1
0.25	60	45	530.45	113.25	20.35	67.97
0.35	40	30	495.62	127.45	20.14	63.47
0.15	60	45	463.23	107.53	22.66	68.56
0.25	80	15	507.6	122.22	19.99	66.94
0.35	80	30	371.12	127.12	21.07	61.06
0.35	60	30	398.74	120.04	20.78	63.08
0.35	80	45	299.48	132.41	21.45	61.45
0.25	40	30	610.6	117.81	19.91	68.42
0.25	80	45	444.75	118.45	22.1	65.43
0.15	80	15	432.48	123.47	21.79	67.22
0.25	40	15	488.12	115.42	20.91	70.38
0.25	60	15	481.78	110.83	20.21	69.93
0.15	80	45	341.98	111.09	26.65	64.62
0.35	80	15	391.27	129.69	19.73	62.49
0.25	40	45	673.7	125.64	18.97	67.72
0.35	60	45	408.71	128.74	20.01	62.94

TABLE VII. Descriptive Statistics — ABS Mechanical Properties.

Property	Min	Max	Mean	Std Dev
Surface Roughness (Ra, µm)	299.48	673.70	459.36	98.18
Impact Strength (J/m)	104.74	141.43	119.15	8.52
Tensile Strength (MPa)	18.97	26.65	21.17	1.57
Hardness (Shore D)	61.06	72.02	66.45	3.04

TABLE IX. Descriptive Statistics — PLA Mechanical Properties.

Property	Min	Max	Mean	Std Dev
Surface Roughness (Ra, µm)	141.20	356.80	256.75	63.73
Impact Strength (J/m)	74.43	90.17	80.93	3.77
Tensile Strength (MPa)	24.70	32.52	29.39	2.04
Hardness (Shore D)	61.36	74.06	69.98	3.04

B. PLA Dataset

TABLE VIII presents the complete experimental dataset for PLA (Polylactic Acid). PLA specimens were processed at 210°C nozzle and 60°C bed temperature. PLA exhibited the lowest surface roughness values overall (141.2–356.8 Ra µm) compared to ABS and PETG, attributable to its low thermal expansion and excellent layer bonding. Impact strength showed a narrow band (74.43–90.17 J/m), and tensile strength ranged from 24.70 to 32.52 MPa — the highest tensile range among the three materials. PLA hardness varied from 61.36 to 74.06 Shore D.

TABLE VIII. Full Experimental Dataset — PLA Material (27 Runs, L27 Full Factorial).

Layer Thickness (mm)	Printing Speed (mm/s)	Infill Density (%)	Surface Roughness (Ra, µm)	Impact Strength (J/m)	Tensile Strength (MPa)	Hardness (Shore D)
0.15	60	30	216.4	78.65	29.58	72.02
0.15	40	45	244.2	79.86	32.52	67.9
0.15	40	30	173.6	78.81	30.72	65.89
0.35	40	15	334.5	82.7	31.97	67.42
0.15	40	15	141.2	81.76	26.98	61.36
0.35	40	45	325.2	87.93	30.21	66.55
0.25	80	30	211.4	77.2	28.12	72.94
0.35	60	15	356.8	81.64	32.51	72.38
0.15	80	30	223.2	75.63	27.25	71.86
0.25	60	30	217.5	79.02	29.34	74.06
0.15	60	15	191.4	80.1	25.94	70.26
0.25	60	45	265.2	83.85	29.26	73.24
0.35	40	30	309.9	82.82	31.73	68.89
0.15	60	45	287.5	81.06	30.98	72.64
0.25	80	15	209.6	74.43	26.7	73.65
0.35	80	30	321.6	80.64	30.85	68.74
0.35	60	30	331.83	83.81	31.55	71.74
0.35	80	45	328.4	89.57	28.89	65.28
0.25	40	30	185.9	78.24	29.94	69.46
0.25	80	45	254.5	81.96	27.85	70.4
0.15	80	15	201.4	77.42	24.7	71.16
0.25	40	15	179.3	79.94	28.4	66.89
0.25	60	15	215.7	78.88	27.53	73.86
0.15	80	45	294.3	80.32	29.01	70.82
0.35	80	15	338.36	77.75	31.34	70.95
0.25	40	45	227	80.94	30.12	69.76
0.35	60	45	346.41	90.17	29.65	69.35

C. PETG Dataset

TABLE X presents the complete experimental dataset for PETG (Polyethylene Terephthalate Glycol). PETG was printed at 240°C nozzle and 80°C bed temperature. PETG exhibited the widest surface roughness range (205.91–595.40 Ra µm), primarily driven by layer thickness, and the highest impact strength values (74.76–122.17 J/m) among all three materials — reflecting its well-known toughness and superior interlayer adhesion. Tensile strength ranged from 17.70 to 25.55 MPa, and hardness from 59.91 to 69.79 Shore D.

TABLE X. Full Experimental Dataset — PETG Material (27 Runs, L27 Full Factorial).

Layer Thickness (mm)	Printing Speed (mm/s)	Infill Density (%)	Surface Roughness (Ra, µm)	Impact Strength (J/m)	Tensile Strength (MPa)	Hardness (Shore D)
0.15	60	30	224.53	83.23	21.17	65.09
0.15	40	45	245.67	91.23	22.2	62.54
0.15	40	30	229.59	81.11	20.88	63.72
0.35	40	15	560.41	95.55	23.11	60.16
0.15	40	15	205.91	84.85	17.7	60.47
0.35	40	45	595.4	94.98	25.55	69.79
0.25	80	30	304.89	85.19	21.34	63.93
0.35	60	15	501.11	114.89	23.89	62.23
0.15	80	30	285.21	74.76	20.95	64.3
0.25	60	30	281.29	89.93	22.23	65.31
0.15	60	15	219.22	90.01	19.62	62.8
0.25	60	45	292.39	94.32	22.98	64.93
0.35	40	30	588.67	87.31	25.23	67.5
0.15	60	45	233.78	88.77	22.45	63.29
0.25	80	15	310.38	108.56	20.14	61.27
0.35	80	30	512.38	98.34	24.65	65.89
0.35	60	30	505.52	96.37	25.11	67.96
0.35	80	45	519.88	97.88	24.97	66.48
0.25	40	30	303.24	84.28	21.91	64.68
0.25	80	45	300.75	86.74	21.87	63.18
0.15	80	15	298.66	86.05	18.78	63.37
0.25	40	15	295.44	90.65	19.92	59.91
0.25	60	15	266.56	99.78	20.39	61.77
0.15	80	45	264.98	77.08	21.62	60.81
0.35	80	15	509.92	122.17	22.71	61.96
0.25	40	45	330.96	93.8	23.54	64.91
0.35	60	45	532.28	101.09	25.42	68.34

TABLE XI. Descriptive Statistics — PETG Mechanical Properties.

Property	Min	Max	Mean	Std Dev
Surface Roughness (Ra, µm)	205.91	595.40	359.96	131.99
Impact Strength (J/m)	74.76	122.17	92.55	10.64
Tensile Strength (MPa)	17.70	25.55	22.23	2.11
Hardness (Shore D)	59.91	69.79	63.95	2.59

D. Cross-Material Dataset Comparison

A comparison of descriptive statistics across the three materials reveals several important trends. PLA achieved the highest mean tensile strength (29.65 MPa), while PETG produced the highest mean impact strength (92.04 J/m), consistent with PETG's known toughness characteristics. ABS exhibited the highest mean surface roughness (465.88 Ra µm), which may be attributed to greater thermal gradient effects during deposition. Hardness values were broadly comparable across materials, with PLA showing marginally higher average Shore D values. The coefficient of variation (CV) for surface roughness was highest for PETG, indicating greater sensitivity to parameter variation — which in turn explains why PETG yielded the highest ML prediction accuracy, as its parameter-property relationships are more pronounced and learnable. These trends align with the ML prediction results in Section IV, where PETG consistently achieved the highest R^2 values across three of the four mechanical properties.

IV. RESULTS AND DISCUSSION

A. ABS Material Results

TABLE II presents the complete R2 values for all eight ML algorithms across all four mechanical properties of ABS material. Cells highlighted in green indicate the best-performing algorithm. ANN achieved the highest accuracy for surface roughness (R2=0.9598), tensile test (R2=0.9719), and hardness test (R2=0.9822). SVR emerged as best for impact test prediction (R2=0.8928). Bayesian Ridge underperformed for hardness (R2=0.8066) and impact (R2=0.6126). BPNN produced severely negative R2 for impact (-0.3806), tensile (-0.8069), and hardness (-1.6378), indicating catastrophic overfitting on the 27-sample dataset [12]. Figs. 1-2 show Actual vs. Predicted plots for the best algorithms on each ABS property.

TABLE II.. R2 Coefficient of Determination -- ABS Material. (* = Best per property)

Property	ANN	SVR	LR	KNN	RF	XGB	Bayesian	BPNN
Surface Roughness	**0.9598**	0.9422	0.9494	0.9271	0.9408	0.9359	0.6857	0.9355
Impact Test	0.8729	**0.8928**	0.8513	0.8462	0.8093	0.8330	0.6126	-0.3806
Tensile Test	**0.9719**	0.9712	0.9664	0.9468	0.9416	0.9238	0.8718	-0.8069
Hardness Test	**0.9822**	0.9803	0.9659	0.9613	0.9498	0.9525	0.8066	-1.6378

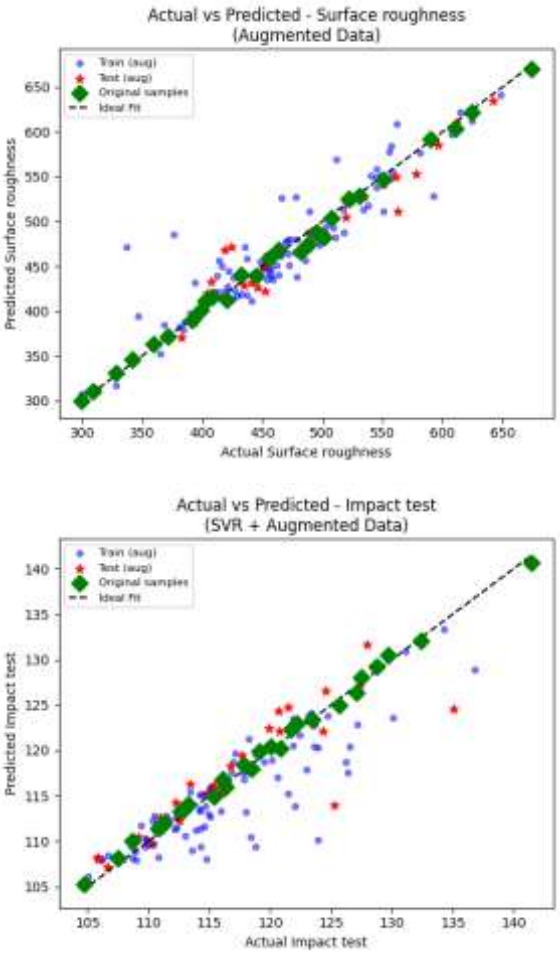

***Fig. 1.**. ABS: ANN -- Surface Roughness (R2=0.9598) [left]; SVR -- Impact Test (R2=0.8928) [right].*

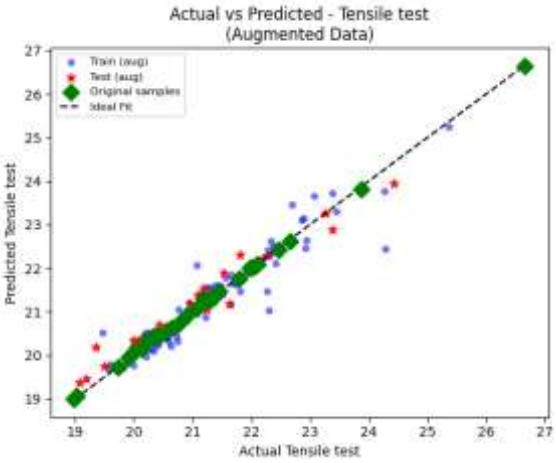

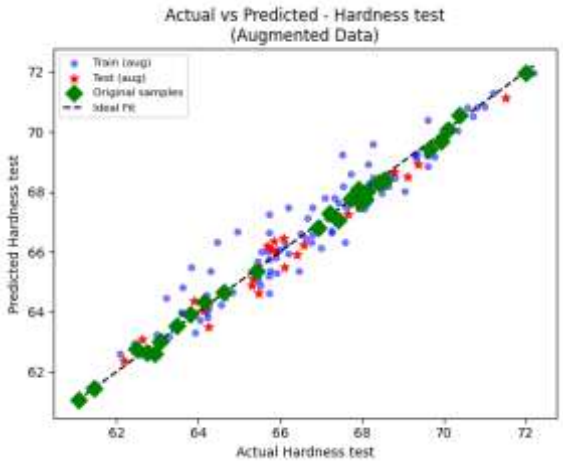

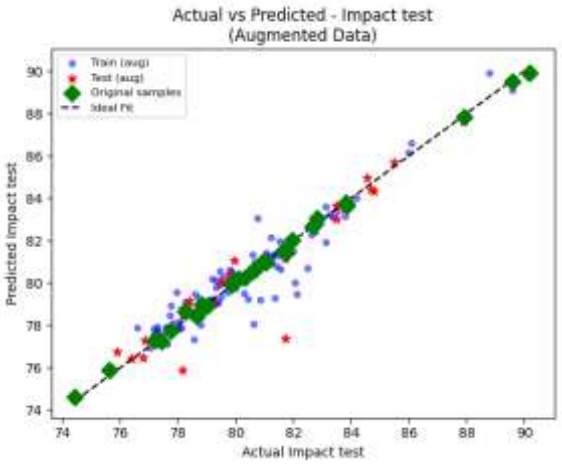

Fig. 2.*. ABS: ANN -- Tensile Test (R2=0.9719) [left]; ANN -- Hardness Test (R2=0.9822) [right].*

Fig. 3.*. PLA: ANN -- Surface Roughness (R2=0.9724) [left]; ANN -- Impact Test (R2=0.9373) [right].*

B. PLA Material Results

TABLE III presents R2 values for PLA material. ANN achieved highest accuracy for surface roughness (R2=0.9724), impact test (R2=0.9373), and tensile test (R2=0.9623). SVR outperformed for hardness (R2=0.9255). PLA yielded generally higher R2 values than ABS across most algorithms, attributable to PLA's more stable thermal behavior, better layer adhesion, and reduced warping. LR achieved competitive R2=0.9708 for surface roughness, suggesting a near-linear parameter-surface relationship. BPNN showed negative R2 for impact and near-zero for tensile due to overfitting.

TABLE III.. R2 Coefficient of Determination -- PLA Material. (* = Best per property)

Property	ANN	SVR	LR	KNN	RF	XGB	Bayesian	BPNN
Surface Roughness	**0.9724**	0.9669	0.9708	0.9669	0.9588	0.9586	0.8131	0.9600
Impact Test	**0.9373**	0.9241	0.9258	0.9308	0.9312	0.9247	0.7810	-0.8032
Tensile Test	**0.9623**	0.9601	0.9598	0.9141	0.8939	0.9059	0.8670	-0.0015
Hardness Test	0.8772	**0.9255**	0.8904	0.8771	0.8821	0.8640	0.4212	-0.5004

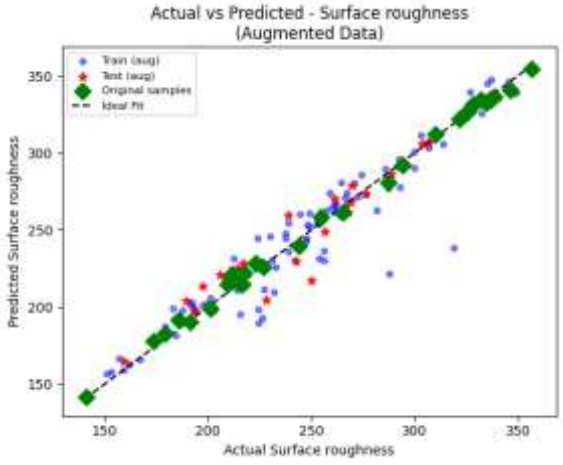

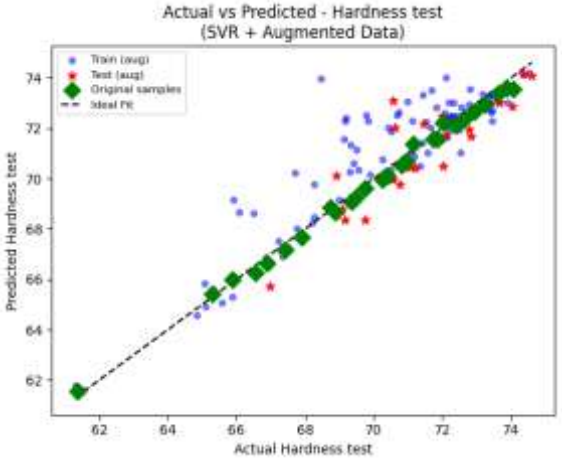

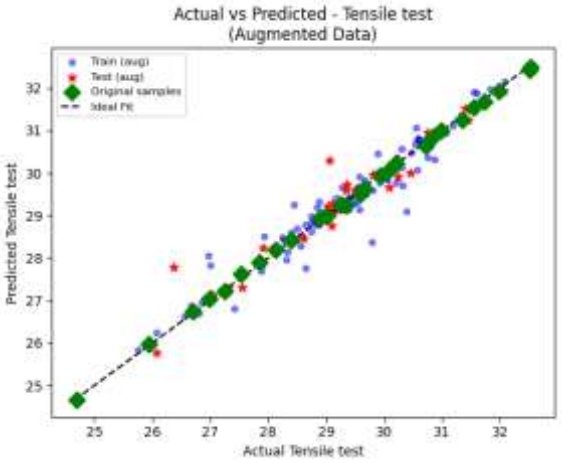

Fig. 4.*. PLA: ANN -- Tensile Test (R2=0.9623) [left]; SVR -- Hardness Test (R2=0.9255) [right].*

C. PETG Material Results

TABLE IV presents R2 values for PETG -- the highest-accuracy material of all three. ANN achieved outstanding performance for surface roughness (R2=0.9739), tensile test (R2=0.9894), and hardness (R2=0.9687). Remarkably, Linear Regression achieved its highest R2=0.9793 for PETG impact test, surpassing both ANN (R2=0.9667) and SVR (R2=0.9741), suggesting near-linear dependence of PETG impact resistance on the input parameters. BPNN showed improved surface roughness prediction (R2=0.9716) for PETG, reflecting more uniform deposition

behavior. Bayesian Ridge remained weakest for hardness (R2=0.7662).

TABLE IV.. R2 Coefficient of Determination -- PETG Material. (* = Best per property)

Property	ANN	SVR	LR	KNN	RF	XGB	Bayesian	BPNN
Surface Roughness	**0.9739**	0.9710	0.9678	0.9663	0.9619	0.9693	0.8772	0.9716
Impact Test	0.9667	0.9741	**0.9793**	0.9746	0.9565	0.9517	0.8517	0.4102
Tensile Test	**0.9894**	0.9831	0.9819	0.9780	0.9748	0.9752	0.9249	0.5400
Hardness Test	**0.9687**	0.9621	0.9608	0.9508	0.9589	0.9084	0.7662	-1.6594

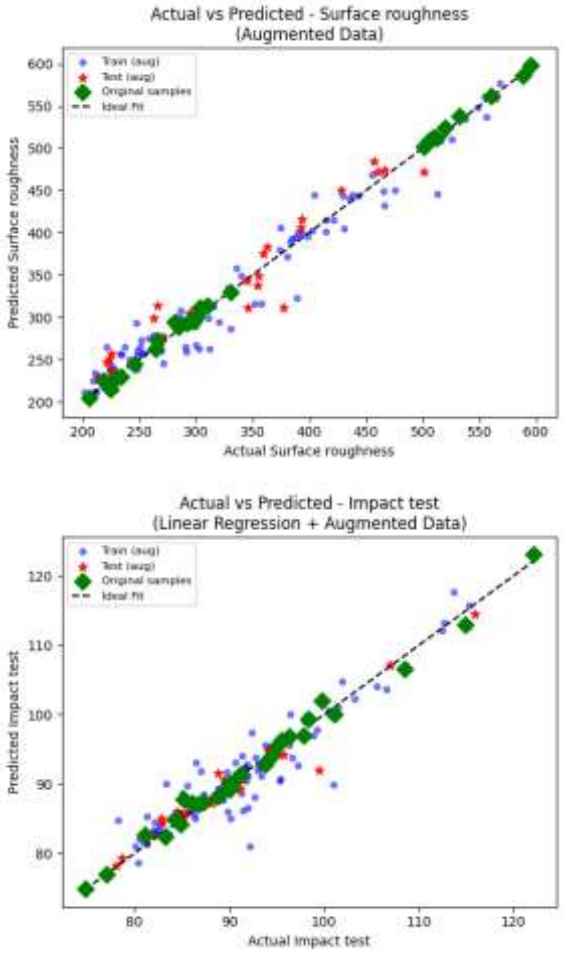

Fig. 5.. PETG: ANN -- Surface Roughness (R2=0.9739) [left]; LR -- Impact Test (R2=0.9793) [right].

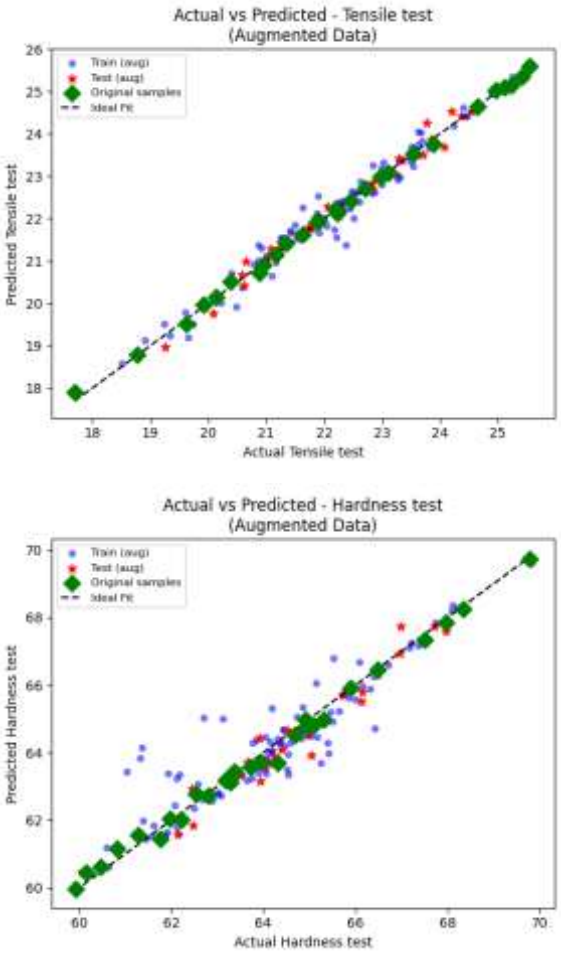

Fig. 6.. PETG: ANN -- Tensile Test (R2=0.9894) [left]; ANN -- Hardness Test (R2=0.9687) [right].

D. Comparative Analysis Across All Materials and Algorithms

TABLE V consolidates the best R2 values per material-property combination. PETG produced the highest best-case R2 in three out of four properties (surface roughness: 0.9739, impact: 0.9793, tensile: 0.9894), while ABS achieved the highest hardness accuracy (R2=0.9822). ANN emerged as the most consistently superior predictor, achieving best R2 in 9 out of 12 material-property combinations. SVR was second-best overall. XGBoost and Random Forest showed reliable R2 above 0.93 for PETG. BPNN showed catastrophic overfitting (negative R2) for ABS and PLA but improved for PETG.

TABLE V.. Best R2 Values Across All Materials and Properties.

Property	Best Algo.	ABS R2	PLA R2	PETG R2	Top Mat.
Surface Roughness	ANN	0.9598	0.9724	**0.9739**	PETG
Impact Test	LR / SVR	0.8928	0.9373	**0.9793**	PETG
Tensile Strength	ANN	0.9719	0.9623	**0.9894**	PETG
Hardness Test	ANN	**0.9822**	0.9255	0.9687	ABS

V. CONCLUSION

This study presented a comprehensive multi-material, multi-algorithm ML-based framework for predicting four mechanical properties -- tensile strength, hardness, surface roughness, and impact strength -- of FDM-fabricated parts across ABS, PLA, and PETG. Key conclusions are: (1) ANN is the most consistently superior algorithm (best R2 in 9/12 combinations), with peak

R2=0.9894 for PETG tensile strength and R2=0.9822 for ABS hardness; (2) PETG demonstrated highest overall ML prediction accuracy across three out of four properties; (3) SVR is the second-best overall performer, particularly effective for ABS impact test (R2=0.8928) and PLA hardness (R2=0.9255); (4) Linear Regression achieved a strong R2=0.9793 for PETG impact test; (5) Bayesian Ridge consistently underperformed for hardness and impact due to its linear model assumption; (6) BPNN produced severe overfitting (negative R2) for ABS and PLA; (7) The ML-based approach substantially reduces the need for extensive physical experimentation, supporting data-driven FDM process optimization.

Future work should expand experimental datasets, incorporate additional FDM parameters, and integrate validated ML models into real-time closed-loop FDM control systems.

ACKNOWLEDGEMENT

The authors gratefully acknowledge the Department of Mechanical Engineering, RVR & JC College of Engineering, Guntur, Andhra Pradesh, India, for providing the computational infrastructure and academic environment supporting this research. Special thanks are due to the open-source community for maintaining Python libraries (scikit-learn, XG Boost, NumPy, Pandas, Matplotlib, Seaborn) used in this study. No external funding was received.

DATA AVAILABILITY

The datasets (ABS.csv, PLA.csv, PETG.csv -- 27 samples each) and all Python notebooks used for model training and evaluation are available from the corresponding author upon reasonable request.

REFERENCES

[1] I. Fidan et al., "Recent Inventions in Additive Manufacturing: Holistic Review," Inventions, vol. 8, p. 103, 2023.

[2] R. B. Kristiawan et al., "A Review on the FDM 3D Printing: Filament Processing, Materials, and Printing Parameters," Open Engineering, vol. 11, pp. 639-649, 2021.

[3] S. Wickramasinghe et al., "FDM-Based 3D Printing of Polymer and Associated Composite: A Review," Polymers, vol. 12, p. 1529, 2020.

[4] M. Algarni and S. Ghazali, "Comparative Study of PLA, ABS, PEEK, and PETG Mechanical Properties to FDM Parameters," Crystals, vol. 11, p. 995, 2021.

[5] C. Wang et al., "Machine Learning in Additive Manufacturing: State-of-the-Art and Perspectives," Additive Manufacturing, vol. 36, p. 101538, 2020.

[6] M. Özkül et al., "Predicting Mechanical Properties of FDM-Produced Parts Using ML Approaches," J. Appl. Polym. Sci., vol. 142, e56899, 2025.

[7] A. Cerro et al., "Use of ML Algorithms for Surface Roughness Prediction of Printed Parts via FDM," Int. J. Adv. Manuf. Technol., vol. 115, pp. 2465-2475, 2021.

[8] N. Hooda et al., "Deposition Angle Prediction of FDM Process Using Ensemble Machine Learning," ISA Transactions, vol. 116, pp. 121-128, 2021.

[9] P. Charalampous et al., "Learning-Based Error Modeling in FDM 3D Printing Process," Rapid Prototyping J., vol. 27, pp. 507-517, 2021.

[10] O. Ulkir, "Conductive Additive Manufactured ABS Filaments: Statistical Approach to Mechanical and Electrical Behaviors," 3D Print. Addit. Manuf., vol. 10, pp. 1423-1438, 2023.

[11] G. D. Goh et al., "A Review on Machine Learning in 3D Printing: Applications, Potential, and Challenges," Artif. Intell. Rev., vol. 54, pp. 63-94, 2021.

[12] S. Kumar et al., "Machine Learning Techniques in Additive Manufacturing: A State of the Art Review," J. Intell. Manuf., vol. 34, pp. 21-55, 2023.

[13] N. A. Fountas et al., "Single and Multi-Objective Optimization of FDM-Based AM Using Metaheuristic Algorithms," Procedia Manuf., vol. 51, pp. 740-747, 2020.

[14] T. Sai et al., "Modeling and Optimization of FDM Process Through PLA Implants Using ANFIS and Whale Optimization," J. Braz. Soc. Mech. Sci., vol. 42, p. 617, 2020.

[15] O. A. Mohamed et al., "Wear Performance of FDM Printed PC-ABS Parts Using ML-Genetic Algorithm," J. Mater. Eng. Perform., vol. 31, pp. 2967-2977, 2022.

[16] O. Ulkir et al., "Raster Angle Prediction of AM Process Using Machine Learning," Appl. Sci., vol. 14, p. 2046, 2024.

[17] A. S. Khusheef et al., "Deep Learning-Based Multi-Sensor Fusion for FDM Process Monitoring," Arab. J. Sci. Eng., vol. 49, pp. 10501-10522, 2024.

[18] Y. Wang et al., "Additive Manufacturing Is Sustainable Technology: Bibliometric Investigations of FDM," Rapid Prototyping J., vol. 28, pp. 654-675, 2022.

[19] P. Badoniya et al., "A State-of-the-Art Review on Metal Additive Manufacturing," J. Braz. Soc. Mech. Sci., vol. 46, p. 339, 2024.

[20] S. Rouf et al., "Additive Manufacturing Technologies: Industrial and Medical Applications," Sustain. Oper. Comput., vol. 3, pp. 258-274, 2022.

[21] L. Zhou et al., "Additive Manufacturing: A Comprehensive Review," Sensors, vol. 24, p. 2668, 2024.

[22] T. Vaneker et al., "Design for Additive Manufacturing: Framework and Methodology," CIRP Annals, vol. 69, pp. 578-599, 2020.

[23] S. Gunes et al., "Application of ANN to Dimensional Accuracy of 3D-Printed PLA Parts," J. Polym. Sci., vol. 62, pp. 1864-1889, 2024.

[24] A. Patel and M. Taufik, "Extrusion-Based Technology in AM: A Comprehensive Review," Arab. J. Sci. Eng., vol. 49, pp. 1309-1342, 2024.

[25] N. A. Fountas et al., "Experimental Investigation of Surface Roughness in 3D-Printed PLA Items Using DOE," Proc. IMechE Part J, vol. 236, pp. 1979-1984, 2022.

[26] J. Kechagias and S. Zaoutsos, "Effects of 3D-Printing Parameters on FFF Parts Porosity," Mater. Manuf. Process., vol. 39, pp. 804-814, 2024.

[27] N. Ben Ali et al., "Experimental Optimization of Process Parameters on Mechanical Properties of 3D Printed Parts," J. Appl. Polym. Sci., vol. 139, 2022.

[28] R. Rai et al., "Machine Learning in Manufacturing and Industry 4.0 Applications," Int. J. Prod. Res., vol. 59, pp. 4773-4778, 2021.

[29] M. Khalil et al., "ML and Statistical Analysis for Forecasting Building Energy Consumption," Eng. Appl. Artif. Intell., vol. 115, p. 105287, 2022.

[30] C. Hu et al., "Fabrication of Long Carbon Fiber Reinforced PLA Composites via FDM: ML Analysis," J. Compos. Mater., vol. 55, pp. 1459-1472, 2021.

[31] K. Tufekci et al., "Stress Relaxation of 3D Printed PLA of Various Infill Orientations," J. Appl. Polym. Sci., vol. 140, 2023.

[32] J. D. Kechagias et al., "Experimental Investigation and NN Development for PMMA Tensile Properties," Int. J. Adv. Manuf. Technol., vol. 134, pp. 4387-4398, 2024.

[33] B. El Essawi et al., "Optimization of Infill Density and Fiber Angle in 3D Printed Carbon-Fiber Nylon," Results Eng., vol. 21, p. 101926, 2024.

[34] J. Zhu et al., "Surface Quality Prediction for 3D Printing With Transfer Learning-Enhanced Gradient Boosting," Expert Syst. Appl., vol. 237, p. 121478, 2024.

[35] G. Prashar et al., "Additive Manufacturing: Expanding 3D Printing Horizon in Industry 4.0," Int. J. Interact. Des. Manuf., vol. 17, pp. 2221-2235, 2023.

[36] H. Ardeshir et al., "A Scientometrics Study for Fused Deposition Modeling," Alexandria Eng. J., vol. 99, pp. 217-231, 2024.

[37] M. Moradi et al., "Experimental Investigation on Mechanical Characterization of 3D Printed PLA by FDM," Mater. Res. Express, vol. 8, p. 035304, 2021.

[38] A. Rasheed et al., "Taguchi Optimization of FDM Parameters for Enhancement of Tensile Properties of PLA-ABS," Mater. Res. Express, vol. 10, p. 095307, 2023.

[39] I. Khan et al., "A Review of Extrusion-Based AM of Multi-Materials-Based Polymeric Laminated Structures," Compos. Struct., vol. 349-350, p. 118490, 2024.

[40] J. M. Gardner et al., "Machines as Craftsmen: Localized Parameter Setting for FFF 3D Printing," Adv. Mater. Technol., vol. 4, p. 1800653, 2019.

[41] N. H. Musa et al., "Influence of Nozzle Temperatures on 316L SS Parts by Material Extrusion," Rapid Prototyping J., vol. 30, pp. 2021-2032, 2024.